Model-based estimation of muscle and joint reaction forces exerted during an abrupt horizontal deceleration task performed by elite athletes

Rodrigo André Bonacho Mateus*
rodrigo11279@gmail.com
Thesis to obtain the Master of Science Degree in Biomedical Engineering
Supervisors: António Prieto Veloso** and Jorge Manuel Mateus Martins *

*Instituto Superior Técnico, Universidade de Lisboa
** Faculdade de Motricidade Humana, Universidade de Lisboa
October 2018

Abstract — Abrupt deceleration is a common practice in several sports, where sudden changes of direction are needed to perform at the highest level. The aim of this work is to estimate muscle forces, joint reaction forces and muscle contributions to the acceleration of the center of mass during a rapid anterior/posterior deceleration task. Six elite male injury free athletes participated in this work. Scaled generic musculoskeletal models, consisting of 10 segments, 23 degrees of freedom and 92 musculotendon actuators were used in OpenSim. Data processing and IK steps were performed in Visual3D. For both SO and CMC, the same adjusted kinematics from RRA were used as inputs to estimate muscle forces. Joint reaction forces were calculated based on the estimated muscle forces from SO. Comparing both methods regarding resultant muscle forces, higher Pearson correlation coefficients (PCC) were shown for uniarticular muscles (PCC = 0.900 ± 0.068), when compared to biarticular muscles (PCC = 0.725 ± 0.174). Regarding joint reaction forces, peak magnitudes observed along the fore – aft direction at the right knee joint (11.961 ± 2.646 BW) and right hip joint (10.260 ± 3.634 BW). The insertion of muscles in the model resulted in force values approximately 10 times higher than if only a multi linked rigid – body model was used. The quadriceps were the main contributors to the mass centre's acceleration profile along the A/P direction, aided by the soleus, counteracted most of the effects applied by gravity along the vertical direction, and finally, along the mediolateral direction, opposed the contribution of the gluteus maximus to maintain the body stable.

Keywords — Abrupt A/P deceleration, Musculoskeletal Modelling, Static Optimization, Computed Muscle Control, Bone – on – bone forces, Induced Accelerations Analysis

I. Introduction

Nowadays, in elite sports, the smallest of details, like a hundredth of a second in timed events, a centimeter in either long or high jump, or even in team sports, such as football, basketball or volleyball, decide every victory. Because of that, the margin of error is decreasing drastically, compelling the athletes to push beyond the limits of their performances, so much so that a myriad of factors besides the physical attributes come into play to gain the upper hand on the competition.

Consequently, it is expected on the athlete's fitness levels to be extremely high, in order to endure the training loads to which they are subjected, as an injury can have severe effects on the aspirations of the individual or, in case of team sports, the aspirations of the team. On the other end, the higher the training loads, the higher the risk of contracting an injury.

Most of the movements are related to accelerations, or decelerations of the body, in order to produce direction changes. Several works focus on the former (Atwater, 1982; Schache, Kim, Morgan, & Pandy, 2010; Veloso, João, Valamatos, Cabral, & Moniz-Pereira, 2015), however deceleration movements are just as important for the success of the athlete. Not only team sports, such as basketball, volleyball and soccer, but also individual sports, like squash, tennis or badminton, require several changes of directions, with constant accelerations and decelerations. With respect to the decelerations, they may occur because of the boundary lines that keep players in game, or as a reaction to other players actions. Hence, decelerations tasks are key to the performance of the athlete in any sport.

The estimation of muscle forces, as well as bone – on – bone forces, in more explosive tasks can be extremely important in rehabilitation and performance enhancement. These forces can be obtained *in vivo* (Bergmann, Deuretzbacher, Heller, Graichen, & Rohlmann, 2001; Renström, Arms, Stanwyck, Johnson, & Pope, 1986), however ethical issues hinder the viability of such methods. An alternative to this is the implementation of musculoskeletal models to obtain these forces (Alvim, Lucareli, & Menegaldo, 2018; Pandy & Zajac, 1991; Pandy, Zajac, Sim, & Levine, 1990). Studying muscle contributions to the accelerations of the centre of mass also presents several findings on how muscles are

summoned during this task, paving the way to create more efficient injury protocols .

OpenSim (S. L. Delp et al., 2007) is an open – source software that allows the joint implementation of a musculoskeletal model and experimental data to perform all the analysis necessary in this. Muscle forces will be estimated using both Static Optimization (SO) and Computed Muscle Control (CMC) (D G Thelen & Anderson, 2006; Darryl G. Thelen, Anderson, & Delp, 2003).

From the literature, the only work focusing on this particular task implements a multi linked rigid body model, with no muscles, to perform an induced accelerations analysis and compute the shear forces at the knee (João, Ferrer, & Veloso, 2018)

The main objectives of this dissertation were to estimate the muscle forces, joint reaction forces and to identify the muscle contributions to the center of mass on elite athletes while performing an abrupt A/P deceleration task. Comparison steps were also taken between two optimization methods for muscle force estimation (Static Optimization and Computed Muscle Control) and between using a musculoskeletal model and a linked rigid – body model to estimate joint reaction forces and perform an induced acceleration analysis

II. Materials and Methods

1) Subjects, Task and Experimental Protocol

In this work, six elite male team sports injury free athletes consented to participated in this study (22 ± 4 years, 183 ± 8 cm, 79 ± 14 kg).

The volunteers executed a series of five abrupt A/P deceleration trials, in which ground reaction forces and kinematic data were recorded. The best one amongst the set of five was chosen.

Kinematic data was collected at 300 Hz using 8 infrared cameras (Oqus 300, Qualisys AB, Sweden) synchronized in time and space with two force plates (Kistler, Switzerland). 28 reflective markers and semi-rigid marker clusters were used to guide an 8 rigid multibody biomechanical model developed using the Visual 3D platform (C-Motion, Inc.).

Anthropometric measures (body mass, stature) and motion capture tests were performed. The passive markers and four marker clusters were placed based on the calibrated anatomical system technique (Cappozzo, Catani, Della Croce, & Leardini, 1995) by the same researcher. Specifically, six markers were placed on the trunk, one on top of each acromion, one on the C7 spinous process, two on the sternum area and one on the spinous apophysis that was aligned with the lower sternum marker (placed so that soft tissue artifact and collinearity was avoided). At the pelvis, two markers were placed on each posterior superior iliac spines and two along each iliac crest. 8 Markers were also placed on the great trochanters head, the lateral and medial femur epicondyles, the lateral and medial ankle malleoli and on the top of the first and fifth metatarsal heads. Each foot had also one marker on the heel. Finally, the mentioned marker clusters were attached to both thighs and shanks.

2) Data Processing and Inverse Kinematics

Kinematic and kinetic variables were low pass filtered using a 4th order Butterworth filter at 8Hz. The biomechanical model built for each participant had 8 segments (feet, shanks, thighs, pelvis and a trunk segment). The local coordinate systems of each segment were defined in accordance with Robertson et al (Robertson, Caldwell, Hamill, Kamen, & Whittlesey, 2014). The hip joint center was computed using the pelvis markers, through a regression equation proposed by Bell et al (Bell, Pedersen, & Brand, 1990), the knee joint center was the mid-point of the epicondyles and ankle joint center the mid-point of the malleoli (Robertson et al., 2014).

The Inverse kinematics (IK) problem was solved as a global optimization problem (Lu & O'Connor, 1999). Segment masses were determined according to Dempster (Dempster, 1955), whereas the remaining inertial parameters were computed based on Hanavan (Hanavan, 1964).

3) Musculoskeletal model and simulations

A 12 segment, 29 degrees of freedom musculoskeletal model was used to create the simulation. Each lower extremity had five degrees-of-freedom. The hip was modeled as a ball-and-socket joint (3 degrees of freedom), the knee was modeled as a custom joint with 1 degree of freedom (Seth et al., 2010), and the ankle was modeled as a revolute joint (1 degree of freedom) (S. L. L. Delp et al., 1990). Lumbar motion was modeled as a ball-and-socket joint (3 degrees of freedom) (Anderson & Pandy, 1999). The lower extremity and back joints were actuated by 92 musculotendon actuators (Anderson & Pandy, 1999; S. L. L. Delp et al., 1990).

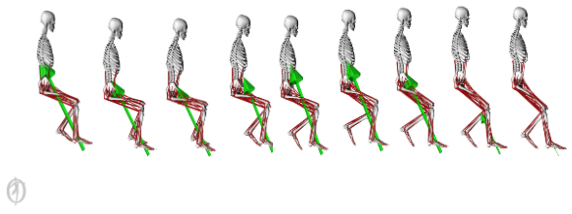

Figure 1. Poses representing the subject AMG attained from OpenSim. The arrow represents the ground reaction forces.

The model was manually scaled to match each subject's anthropometry using previously attained scale

factors for the model segments. The mass was scaled preserving mass distribution among body segments.

A residual reduction algorithm (RRA) step (Anderson, John, Guendelman, Arnold, & Delp, 2006) was inserted in the workflow to minimize errors related to kinematic inconsistencies and modelling assumptions. RRA makes adjustments to the location of the centre of mass, to the mass of the segments in the model, and to the experimental kinematic data. Positional errors were kept within a range of acceptable values (< 5 cm for translational and <5° for angular degrees of freedom). After the first passage, RRA tracking weights related to the degrees of freedom for smaller errors between experimental data and the adjusted kinematics were lowered. Several RRA iterations were performed until the residual forces and torques converged. Joint moments obtained from RRA were compared to inverse dynamics (ID). Optimizer derivative step size and convergence tolerance were set to 10^{-4} and 10^{-5}, respectively. The subtalar and metatarsophalangeal joints were locked in a neutral position.

The adjusted model was used for estimating muscle forces during the task using the SO and CMC optimization methods. At the implementation of OpenSim SO, maximum values for residuals, called optimal forces, were set at 20 N for residual forces and 20 Nm for residual torques, the minimum values that allowed the simulation to run smoothly. CMC uses a proportional derivative controller to provide kinematics feedback to adjust model position during the simulation. Moreover, in CMC, the sum of squared actuator controls plus the sum of desired acceleration errors is minimized, while for SO, only the sum of squared actuator controls is minimized. Different from SO, the CMC algorithm allows constraining the residuals directly, which are set the same way as they were for RRA. Muscle force–length–velocity properties were taken into account and a Hill-type muscle model was used in this final step. The Pearson correlation coefficient (PCC) was used to quantify the similarities between force estimations using CMC and SO.

Bone – on – bone forces were calculated using the JointReaction analysis, available in OpenSim (S. L. Delp et al., 2007). The forces obtained from SO and the adjusted kinematics from RRA were used for this analysis. Moreover, muscle and gravity contributions to the acceleration of the centre of mass were estimated via an induced accelerations analysis, also available in OpenSim (S. L. Delp et al., 2007). The controls and states obtained from CMC were used to compute these contributions. A rolling constraint without slipping was inserted in this analysis to substitute the interaction of the musculoskeletal model with the surrounding environment.

III. Results

To facilitate the analysis of the results, each subject is represented with a line colour and and dash type, as it is shown in table 1. In some of the graphics, the results are represented in terms of the respective subject's body weight, which will also be duly noted in the table below. All the subjects that volunteered for this work used the right leg as the dominant leg to perform this task.

Table 1. Subjects height, mass, graphic features and the task percentage at direction change (%)

Subject	Height (cm)	Mass (Kg)	Task Percentage at direction change (%)	Line Colour and Dash type
AMG	180.0	94.7	49.03	
IMG	180.0	77.0	53.70	
MEB	180.0	63.0	52.18	
MVM	186.7	65.7	79.05	
ND	186.7	92.7	48.05	
OMM	186.7	80.9	53.85	

1) Joint Kinematics and Joint Moments

During this movement, the right hip remains constantly flexed and abducted. For the majority of the task, the right hip stays in a state of external rotation. The motions of the hip are acccompanied by a posterior tilt along the sagittal plane (with varying angles between subjects) and a posterior pelvis rotation to the contralateral side along the transverse. As for the pelvis kinematics along the coronal plane, it moves towards a downwards pelvic rotation, with varying angles between subjects. In order to dissipate as much as possible the impact forces occurring during this task, the knee joints stays flexed and the ankle joint in dorsiflexion. The lumbar joint stays extended, tilted to the side of the supporting leg and in contralateral lumbar rotation.

The net internal joint moments obtained from inverse dynamics are caused by the action of internal forces, which results in moments across a joint axis, and balance out the moments created by forces acting externally to the rigid body, creating moments across the same joint axis. Hence, it is expected that the curves of the joint moments along each of the available anatomical planes at a particular joint contradict the general behaviour of the correspondent kinematic data.

2) Residual Reduction Algorithm

RRA increases consistency with the ground reaction force data of the model and kinematics, by minimizing the residual forces and torques that are inserted in the model to account for modelling assumptions and dynamic inconsistencies. As expected, the reduction in residual forces was much more evident than the reduction observed in the residual torques. Observed reductions in peak residual forces were, on average, 86% along the fore – aft direction (FX), 71% along the vertical direction (FY) and approximately 80% along the mediolateral direction (FZ). Regarding the peak residual moments, reductions, on average, reached 40% for the pelvis list (MX), 31% for the pelvis rotation (MY) and 10% pelvis tilt

(MZ). Concerning the root mean square (RMS) across subjects, for the residual forces and torques, larger values were obtained for FX (67.335 ± 33.918 N), FY (87.095 ± 52.794 N) and MZ (102.365 ± 49.434 Nm), corresponding to the predominant translations and torques required for this task. Much smaller values were attained for FZ (15.002 ± 5.542 N), MX (33.563 ± 13.278 Nm) and MY (26.283 ± 5.893 Nm).

3) Muscle Forces

The muscles which exerted larger amounts of force during the task were the *gluteus maximus*, *vasti,* hamstrings and *erector spinae*. This goes along with the fact these muscles are related to the joint moments with the highest magnitude presented in this work: Hip, Knee and Lumbar extensor moments.

0-25Nm), suggesting that the simulation was successful.

To compare both methods for muscle force estimation, a Shapiro–Wilk test and a Kolmogorov–Smirnov test were employed to test both curves for normality, which it was. Thereafter, a Pearson correlation coefficient (PCC) was calculated between the estimations using SO and CMC. For the *gluteus maximus* (0.980 ± 0.013), *vasti* (0.993 ± 0,005), *soleus* (0.957 ± 0,040) and *erector spinae* (0,990 ± 0,004), both methods produced extremely similar muscle force estimations. On the other hand, for the hamstrings (0,881 ± 0,088) and *rectus femoris* (0,546 ± 0,279), although still acceptable, show smaller correlation coefficients.

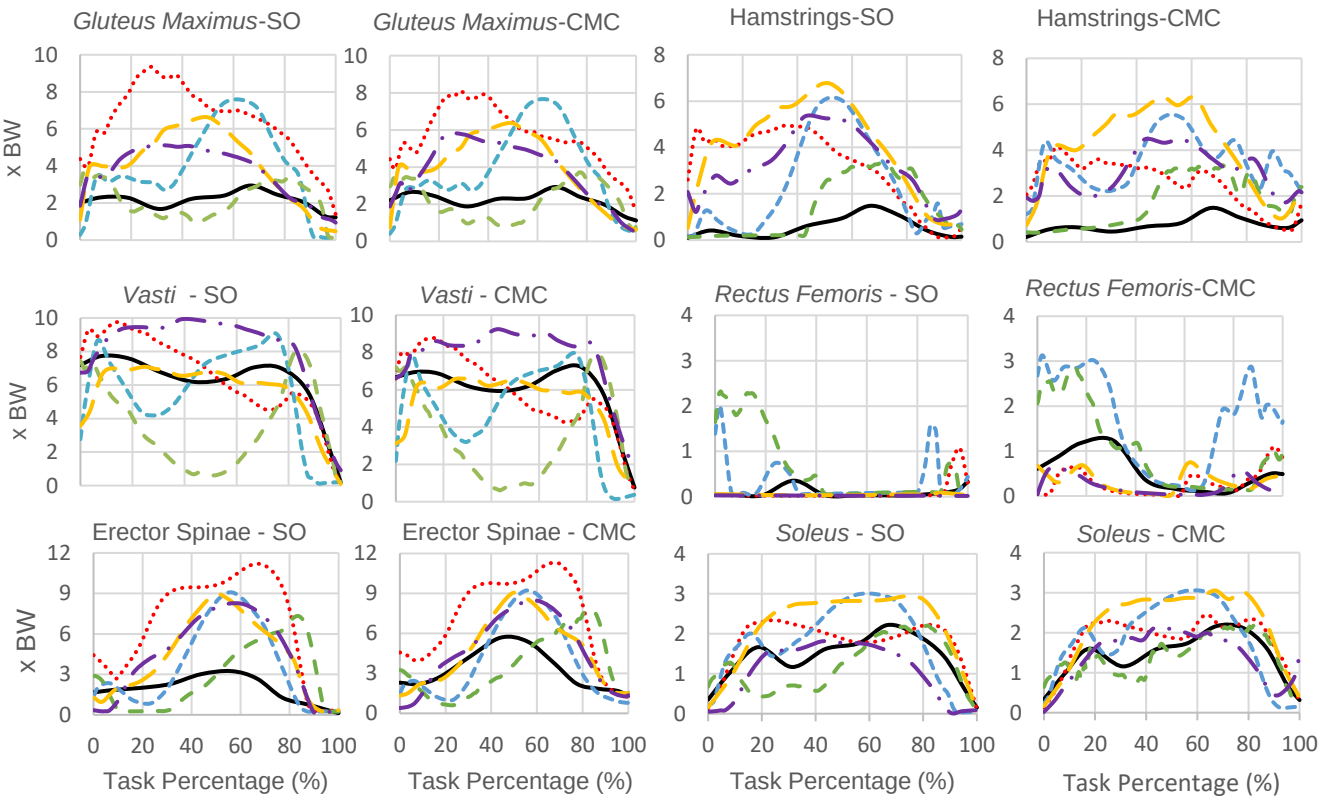

Figure 2. Resulting muscle forces obtained for all the subjects in this work from SO and CMC. The layout for this set of plots goes as follows: First row – SO and CMC results for the *Gluteus Maximus* and Hamstrings; Second row – SO and CMC results for the *Vasti* and *Rectus Femoris* ; Third row – SO and CMC results for the *Erector Spinae* and *Soleus*. The plots for the *Erector Spinae* represent the sum of the muscle forces of the right and left *Erector Spinae*.

The reserve actuators have little to no effect on the estimation of the muscle forces using SO, since their intensity is too small to be accounted as significant. Regarding CMC, from the values obtained for the reserve actuators, one can see that higher values of reserves were obtained for the degrees of freedom related to the right hip, however they land between the acceptable values given by OpenSim (Maximum value for a reserve:

Table 2. Pearson Correlation Coefficient (PCC) between SO and for each muscle

Muscles	AMG	IMG	MEB	MVM	ND	OMM
Gluteus Maximus	0.962	0.984	0.989	0.968	0.997	0.982
Vasti	0.990	0.994	0.997	0.998	0.986	0.992
Hamstrings	0.821	0.922	0.740	0.951	0.972	0.882
Right Erector Spinae	0.978	0.991	0.987	0.932	0.988	0.992
Left Erector Spinae	0.984	0.995	0.992	0.993	0.985	0.990
Soleus	0.990	0.936	0.992	0.923	0.996	0.906
Rectus Femoris	0.404	0.729	0.551	0.962	0.147	0.480
Gastrocnemius	0.892	0.875	0.634	0.752	0.497	0.830
Tibialis Anterior	0.578	0.045	0.876	0.198	0.552	0.772

4) Bone – on – bone Forces

Bone – on – bone forces represent the loads acting at a certain joint to counteract the effects of muscle forces, net joint moments and ground reaction forces on the same joint.

In order to validate the results obtained, two criteria were applied. Firstly, the pelvis joint should not apply any loads between the ground and the pelvis. Secondly, the moment components of the joint reactions loads at the hip and see if they are zero. From the results of the simulations, no loads are applied between the ground and the pelvis. With respect to the second criterion, the moment components are not zero, however they are approximately 3 to 4 orders of magnitude smaller than the other moment components along the other joints, thus they may be looked over.

Starting with the hip joint, one can see that shear forces along the anterior direction are applied on the femur head to nullify the forces created by the lower limb muscles that act upon this joint, which, in this situation, one of the main muscles responsible is the gluteus maximus. These bone – on – bone forces prevent the femur head to penetrate the acetabulum. Large magnitudes for these forces are observed, with peak values ranging from around 6 (AMG) to 14 (IMG and ND) times the body weight of each athlete, located at the time points of the task corresponding to the braking phase of the motion and the direction change point, when the athlete leaves the force platform.

Regarding the vertical direction, compressive forces applied downwards on the femur are depicted during the entirety of the task. Magnitudes are slightly lower than the forces observed along the A/P direction, with peaks varying from approximately 3 (AMG) to 9 (MEB) times the body weight of the athlete. Going over to the knee joint, along the A/P direction, shear forces along the anterior direction are plotted, with the highest magnitude observed at any of the joints, with peak forces reaching 15 times the body weight of the athlete (OMM and IMG). Compressive downwards forces along the vertical direction are also observed by the signal and magnitudes of these forces along the vertical axis, with peak values falling between 5

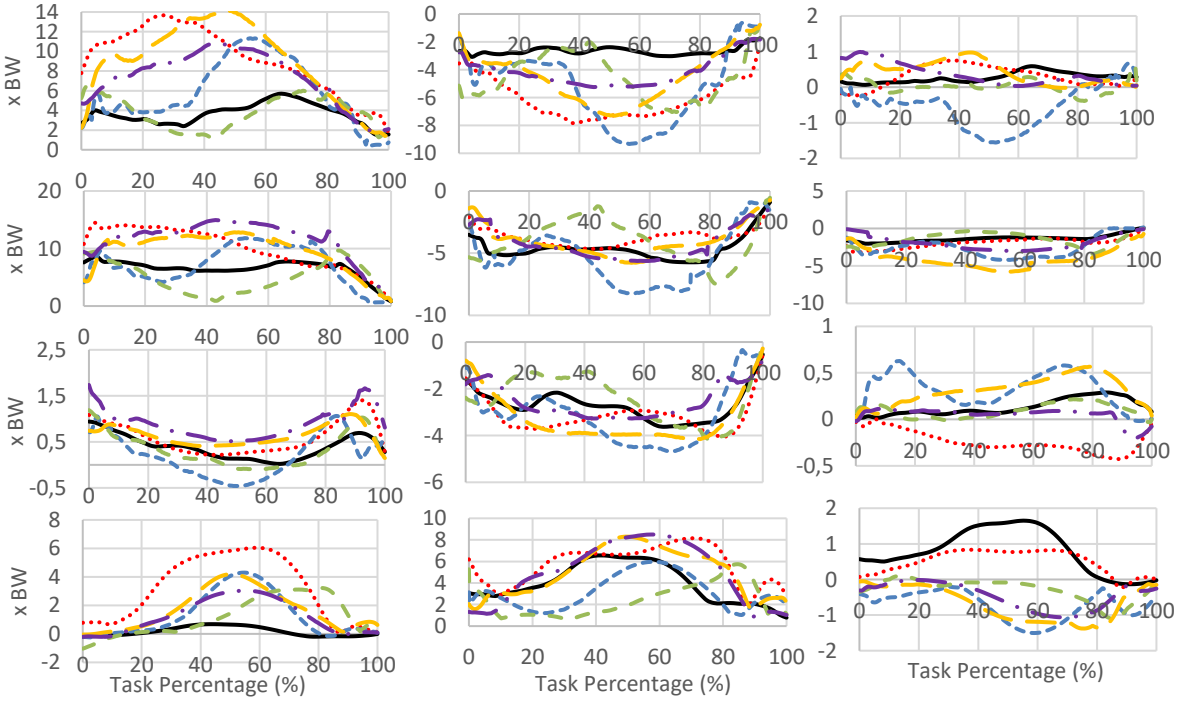

Figure 3. Bone – on – bone forces acting upon the right hip (first row), knee (second row), ankle (third row) and sacroiliac joints (bottom row). The left column refers to the forces acting along the A/P direction, the middle column to the vertical direction and the rightmost column to the mediolateral direction. Values for force are given in terms of body weight (BW) of the respective athlete.

(IMG) and 8 (MEB) times the body weight of the athlete.

Going further down the lower limb, the ankle joint forces represented above comprise the forces applied on the right talus to sustain the application of muscle forces and ground reaction forces on such joint. Forces along the A/P reveal a shape that is concordant with the task in hand, showing peak forces along anteriorly directed during the initial phase of the braking stage and during the propulsion phase regarding the change of direction. A similar behaviour is shown along the vertical direction, albeit with larger magnitudes, with compressive forces reaching almost five times the body weight of the subject (MEB).

Finally, lumbar joint reaction forces are also presented, and show shear forces applied on the torso along the anterior direction, showing a peak magnitude of 6 times the body weight of the participant (IMG) and traction forces along the vertical direction (overall peak magnitudes observed in ND, OMM and IMG of 8-9 x BW).

To study what is the effect of adding muscles to a model, shear bone – on – bone forces acting at the right knee along the fore – aft direction when using a musculoskeletal model and a linked rigid – body model were put against each other and both are shown in figure 4. From observing the figure above, one can depict that, when inserting muscles into the equation, the resulting bone – on – bone forces are around ten times higher that if only net joint moments and ground reaction forces are taken into account. The force profiles are similar for the both cases.

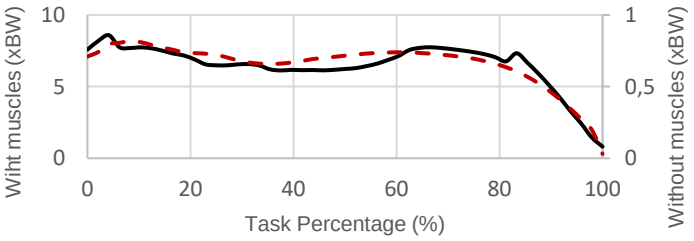

Figure 5. Shear bone – on – bone forces acting at the right knee along the fore – aft direction when using a musculoskeletal model and a linked rigid – body model put against each other. The representative subject was AMG. The left axis corresponds to the forces depicted by a musculoskeletal model, whereas the right vertical axis corresponds to the forces calculated using a linked rigid – body model. The force magnitude are given in terms of body weight (xBW).

5) Induced Accelerations Analysis

In order to analyze the how well the results recreate the contributions of the muscles and gravity to the acceleration of body's center of mass, comparisons between the total acceleration of the body's center of mass along all three directions and the combined contributions of gravity and the muscles present in the model.

From figure 5, one can observe that they match up very well, with slight differences being more visible along the mediolateral direction regarding the shape and magnitude, however this specific contributions are quite smaller when compared to the other contributions along the A/P direction and along the vertical direction.

Along the fore – aft direction, gravity shows a very small contribution when compared to the net contribution of all the muscles, opposing progression along with the contribution from the muscles throughout the entire task. Regarding the vertical direction, gravity propels the body towards the ground, with intensities slightly lower than the normal value for the acceleration of gravity (9.861 m/s^2), which may be representative of the passive resistance created by the rigid bodies in the model. In this direction, muscles contribute to counteract the effect of gravity along this direction so that the model does not subside. Concerning the mediolateral direction, gravity acts to oppose the progression of the center of mass to the right

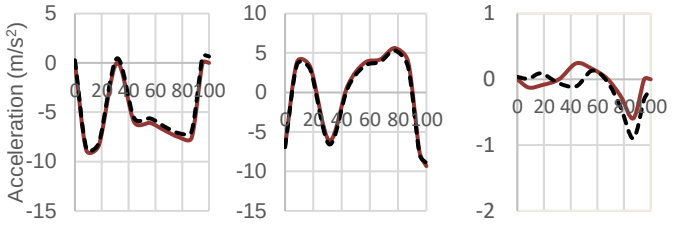

Figure 4. Accelerations for the centre of mass, given in m/s2. The black curve corresponds to the total acceleration and the brown curve corresponds to the accelerations induced by the muscles and gravity. The horizontal axis corresponds to the task percentage. The left plot corresponds to the fore – aft direction, the middle plot to the vertical direction and the right plot to the mediolateral direction.

side of the model during the first 30% of the task and between 50% and 65%, however the net contribution of the muscles far outweigh the contribution of gravity.

The quadriceps (*vasti* + *rectus femoris*) are the protagonist regarding the acceleration of the body's mass center along the anterior/posterior direction. This muscle group is key during both the braking and the direction change periods. Concerning the vertical direction, three muscles groups can be depicted as the main participants in counteracting the effects of gravity on the mass center. They are, once again, the quadriceps, however the soleus also plays a major role, and, in a lower extent, the *gluteus maximus*. Along the mediolateral direction, for the first 30% of the movement, the quadriceps and *gluteus maximus* have approximately equal contributions in magnitude, but opposite in the direction, with the quadriceps propelling the center of mass towards the right side and the *gluteus maximus* annulling this contribution by pushing the center of mass towards the side of the contralateral leg, stabilizing the body to perform this unilateral task. Throughout the task, the hip abductors, such as the *gluteus medius*, also play a role in maintaining the hip in an abduction state. The *gluteus maximus* is the main contributor to the final peak occurring during the last 20% of the task, as the body propels backwards and slightly towards the left side, in order to maintain balance.

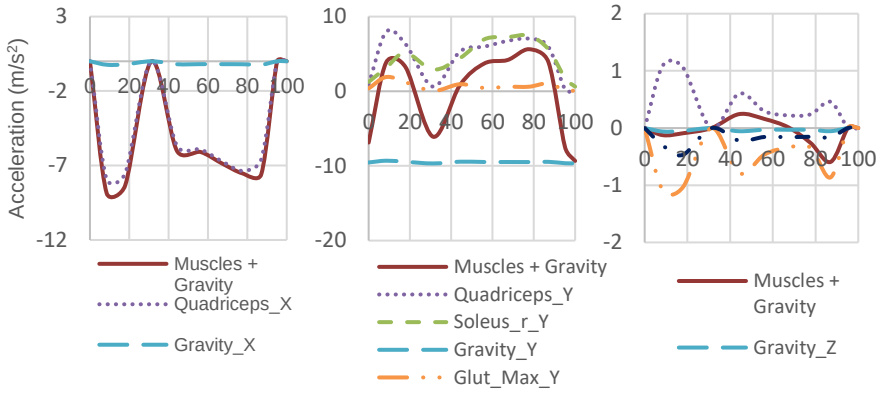

Figure 6. Main contribution of individual muscles to the accelerations of the body's centre of mass along all three directions. The horizontal axis corresponds to the task percentage. The vertical axis gives the accelerations magnitudes, in m/s^2. The left plot corresponds to the fore – aft direction, the middle plot to the vertical direction and the right plot to the mediolateral direction.

IV. Discussion

The novelties and aims inserted in this dissertation were the estimation of muscles activations and forces during an abrupt A/P deceleration task in a healthy group of elite athletes, the estimation of bone – on – bone – forces, and the main contributions for the acceleration of the center of mass. Muscle forces were estimated using two optimization methods (SO and CMC), joint reaction forces were computed using the results from SO and an induced accelerations analysis was performed using the results from CMC. Besides this, additional comparisons between SO and CMC regarding the muscle prediction ability and between the estimation of joint reaction forces using a musculoskeletal model and a rigid – body model.

Previous studies also estimated muscle forces using both of these methods for gait and running (Lin, Dorn, Schache, & Pandy, 2012), single – leg triple hop test (Alvim et al., 2018) and single – leg hop landing (Mokhtarzadeh et al., 2014). This dissertation builds upon these previous works by widening the scope of analysed movements.

The results obtained for both SO and CMC showed similar profiles and magnitudes regarding muscles, such as *the gluteus maximus*, *vasti*, *erector spinae* and *soleus*, whilst for the rest of the muscles presented, which are the *rectus femoris* and hamstrings, slight differences are depicted, which can be explained by two different reasons. Firstly, regarding biarticular muscles, like the *rectus femoris* and hamstrings, CMC estimates higher forces than SO, possibly due to the planar knee model implemented in this simulations, which only requires the attainment of muscle forces along the sagittal plane.

In addition to this, the fact that SO does not take into account muscle activation dynamics may be a significant drawback for explosive tasks such as the one being studied in this work. Secondly, SO only needs to provide a set of muscle forces that will satisfy the net joint moments, kinematic properties and ground reaction forces of the task, so it will tilt towards the muscles with higher maximum isometric force to perform to get the end results. Hence, muscles such as the *tibialis anterior* may suffer from this and result in higher muscle force estimate using CMC, as it was observed. The large values for the force estimates taken for the muscles is representative of the explosiveness inherent to the task being analyzed. For both SO and CMC, force – length and force – velocity relationships of the muscles were taken into account.

Gluteus maximus, in this task, works as a stabilizer by supporting both the HAT segment and pelvis upon the femur head during the entirety of the task and by eccentrically controlling the forward bending motion of the HAT segment. Co – contraction is observed around the knee joint, as both the *vasti* and hamstrings work together to stabilize the knee joint. *Vasti* also provides support by absorbing the impact of the braking portion of the task, by offsetting the action of the knee flexion activity from the hamstrings and by aiding in the final stage of the movement. Validating these inferences, studies showed similar findings for single – leg triple hop test (Alvim et al., 2018), jumping (Pandy & Zajac, 1991) and running (Hamner & Delp, 2013). *Rectus femoris* operates largely as a hip flexor during this task, leaving the *vasti* to be the main knee extensor during this task.

Concerning the *soleus*, one of the main plantarflexors of the foot, works, along with the *vasti*, to absorb the impact

of the braking phase, mainly by preventing the anterior translation of the tibia.

With respect to the *erector spinae*, they play a major role in lumbar rotation, aided by the internal and external obliques. Consequently, they also participated in hip rotation as well as hip flexion. They also provided support in keeping the back of the athletes straight throughout the whole task. All athletes showed an ipsilateral side lumbar bending during the movement, largely performed by the left internal obliques.

According to Lin et al (Lin et al., 2012), SO is the more robust and efficient of the two methods for muscle force estimation, however using SO for high-velocity tasks that require large amounts of force might not be the best of choices. After comparing the two, and since there is still no general agreement on which is the ideal optimization method to be used, SO results were used to compute the bone – on – bone forces occurring in the musculoskeletal model.

From the literature, hip contact forces for walking up and downstairs (Heller et al., 2001) reach average peak magnitudes of 2.51 BW and 2.6 BW, respectively, far below from the values obtained in this work. These values were obtained using an instrumented implant. Moreover, for walking at different speeds, peak values varied between 4.37 BW at 3 km/h and 5.74 at 6 km/h, and for running at different speeds, peak values ranged from 7.49 at 6 km/h to 10.01 BW at 12 km/h (Giarmatzis, Jonkers, Wesseling, Van Rossom, & Verschueren, 2015). These results were obtained for subjects with an average mass of 65.7 Kg, much lower than the average mass of all the participants in this work. These values were attained using the same 23 degrees of freedom, 92 musculotendon actuators musculoskeletal model. In addition to this, hip contact forces were also measured for a stumbling motion using instrumented implants and recorded forces with peak magnitudes that may reach values higher than 8 BW (Bergmann, Graichen, & Rohlmann, 2004).

Several studies computed these forces at the knee joint. Compressive bone – on – bone forces reached peak magnitudes of 6.7 BW during squatting or 6.3 BW while performing a leg press exercise, whilst shear forces peaked at 2.1 BW and 2 BW, respectively. This study was performed on 10 healthy male subjects with an average weight of 93 Kg (Wilk et al., 1996). A different study, performed in 1995, also estimated bone – on – bone forces during loaded and unloaded gait, reporting average peak forces of 5.61 BW and 4.55 BW, respectively (Simonsen, Dyhre-Poulsen, Aagaard, Sjøgaard, & Bojsen-Møller, 1995).

Concerning the ankle bone – on – bone forces, the previously stated study that estimated these forces for loaded and unloaded gait, also calculated the ankle joint bone – on – bone forces, with average peak values of 5.4 BW during 20 Kg loading conditions and 4.18 BW for unloaded conditions.

The lower back bone – on – bone forces were also presented in this work, reaching peak magnitudes of 6 BW (IMG) along the A/P direction, 8.5 BW (OMM) along the vertical and 1.65 BW (AMG) along the mediolateral direction.

From comparing the results with the literature, one can see that the estimation of these forces using musculoskeletal modelling is still not a common approach, much less analysing them in elite athletes and along all the axis. As expected from this task, the joint reaction forces at the knee and hip are the highest along the A/P direction, with all being applied anteriorly on the tibia and femur, respectively, as they are the main contributors to both the braking and the change of direction stages of the task. The largest forces along the fore – aft direction were recorded at the knee, which may be related to the fact that the muscles that exerted the most force in this task, *vasti*, are inserted in this joint. In addition to this, the large hip bone – on – bone forces would result in the bending of the distal portion of the femur (Bergmann et al., 2004), applying even more force on the knee joint, in order to maintain structural integrity of the rigid bodies in the model. Compressive forces along the vertical directions are applied downwards at hip, knee and ankle joints. Traction forces along the vertical directions applied at the sacroiliac joint (lower back) arise from the extension of the back while performing this, as the *erector spinae* and the other lumbar muscles generate forces to resist this extension tendency, thus maintaining balance. These forces may occur as a way for the body to not overload the ankle joint during this task. Following the same line of thought, shear forces along the anterior direction are also observed at the sacroiliac joint. Along the mediolateral direction, where the lowest magnitudes for the hip, ankle and sacroiliac joints were observed, there is much more variability in the directions along which these forces are being generated, which might be a by-product of the difference in strategies employed by each athlete in performing the task. At the knee joint, the bone – on – bone forces along the mediolateral direction are also key to the realization of the task, as they help maintaining the knee in a neutral position.

An additional comparison was also performed to analyse the differences in knee shear joint reaction forces profiles and magnitudes whilst using of a musculoskeletal model and a linked rigid – body model, without accounting for muscle forces. From the results, one was able to depict very similar force profiles, although the differences between force magnitudes are quite large. By using a musculoskeletal model, shear joint forces applied at the knee were 10 times larger than by using a linked rigid – body model (João et al., 2018), showing that muscle forces are the main contributors for the bone – on – bone

forces obtained in this dissertation. A study, performed in 2013 on 1 elite baseball athlete, corroborated this findings (Chen, Andersen, Rasmussen, Tang, & County, 2013).

In the results of IAA, although small, the contribution of residuals to acceleration of the centre of mass might be closely related to the modelling assumptions inserted in this musculoskeletal model – i.e. not incorporating the arms in the model.

Thereupon, regarding the contributions of gravity along the three directions, as expected, it had a much larger contribution along the vertical direction. Concerning the muscles, the quadriceps contribute the most out of every muscle to the acceleration of the body's mass centre along the fore – aft direction. Along the vertical direction, the main knee extensors muscles (quadriceps), the main plantarflexor (*soleus*) and the *gluteus maximus* contribute the most to counteract the effect of gravity on the acceleration of the center of mass. Along the mediolateral direction, the contributions of the quadriceps *and gluteus maximus* balance each each other out through the first part of the task. The *gluteus maximus* is the main contributor to the final peak occurring during the last 20% of the task, as the body propels backwards and slightly towards the contralateral side, in order to maintain balance. Also, larger accelerations values were obtained along the fore – aft direction, which was expected by the larger values of the bone – on – bone forces along such direction.

The findings reported in this part of the dissertation are in agreement with the results obtained from using a linked rigid – body model without muscles, with the knee joint moments being responsible for the majority of the A/P deceleration experienced in this task and the knee and ankle joint moments working together to contribute the most to the vertical acceleration of the body's center of mass (João et al., 2018). This comparison was also performed in a different study using one male elite sprinter (Veloso et al., 2015). Although a different representative subject was used, the same conclusions can be depicted, showing similarities between subjects.

V. Conclusions

To begin with, the musculoskeletal model used in this work is a valid option to portray reliable results in this work. Also, performing multiple passages of RRA prior to the other steps in this work revealed to be key to minimize the effect of kinematic inconsistencies and modelling assumptions.

Furthermore, muscles synergies are in agreement with the joint moments and measured kinematic data. Both SO and CMC predicted similar results in terms of force profile and magnitudes during an abrupt A/P deceleration task, albeit caution must be taken when biarticular muscles, such as the hamstrings or gastrocnemius, are concerned. Moreover, bone – on – bone forces suggest that the muscles are the main contributors to these types of loads applied at the joints. Comparisons between using a linked rigid – body model and using a musculoskeletal model to compute such forces corroborate the previous statement. The effect of taking into account muscle forces in the computation of such forces is visible not only along the vertical direction, but also along the fore – aft direction and mediolateral direction. Largest values for bone – on – bone forces along the anterior direction are observed at the knee.

Finally, the results obtained from the induced accelerations analysis step revealed that the combined contributions from gravity and muscles accounted for almost the totality of the model's centre of mass acceleration. The accelerations along the fore – aft are almost entirely induced by the quadriceps. Regarding the vertical direction, a joint effort mainly between the quadriceps and soleus, with the gluteus maximus contributing in a lesser extent is also depicted. Equivalent findings, where a linked rigid – body model with no muscles was used, corroborate these results, which translates in the fact that the pipeline used in this work provided reliable and insightful results on the individual muscle contributions to the accelerations of the body's centre of mass.

This work may carry some limitations, which could reduce the viability of the results obtained.

To begin with, even though the model implemented in this work is a valid choice to perform all of these analysis, it is still a simplified representation of a real body. Not only that, but also muscle parametres, such as optimal fibre length, tendon slack length or even maximum isometric force might not entirely correspond to their true values, as they were obtained from experiments with different setups and on subjects with different body types than the ones this study analysis.

Although, for this work, 6 elite athletes took part in it, which is a considerably larger sample than other studies performed on this type of subjects, it is still not enough to generalize the findings of these analysis.

Moreover, there is no way to validate the results, due to the lack of EMG data. An ideal situation to corroborate the finding on this work would be to measure the muscle forces, as well as bone – on – bone forces in vivo, however it carries several ethical implications regarding the invasive nature of this technique. Lacking this validation method, although small, there is a possibility that the muscle forces profiles and magnitudes are incorrect or do not correspond entirely to reality.

VI. Future works

Firstly, the loadings on the knee ligaments and their contributions are interesting unknowns that may be extremely important, due to their implications on injury prevention and performance enhancing programs.

Secondly, in order to verify how the body adjusts to injury when performing an abrupt A/P deceleration task,

studying muscle contributions, muscle forces and bone – on – bone forces on athletes that suffered ligament injury or muscle strains would be beneficial to injury prevention programs.

VII. References

Alvim, F. C., Lucareli, P. R. G., & Menegaldo, L. L. (2018). Predicting muscle forces during the propulsion phase of single leg triple hop test. *Gait and Posture*, *59*(July 2017), 298–303. https://doi.org/10.1016/j.gaitpost.2017.07.038

Anderson, F. C., John, C. T., Guendelman, E., Arnold, A. S., & Delp, S. L. (2006). SimTrack: Software for Rapidly Generating Muscle-Actuated Simulations of Long-Duration Movement. *International Symposium on Biomedical Engineering*, 3–6.

Anderson, F. C., & Pandy, M. G. (1999). A dynamic optimization solution for vertical jumping in three dimensions. *Computer Methods in Biomechanics and Biomedical Engineering*, *2*(3), 201–231. https://doi.org/10.1080/10255849908907988

Atwater, A. E. (1982). Kinematic Analysis of Sprinting. *Track and Field Quarterly Review*, *82*(2), 12–16.

Bell, A. L., Pedersen, D. R., & Brand, R. A. (1990). A comparison of the accuracy of several hip center location prediction methods. *Journal of Biomechanics*, *23*(6), 617–621. https://doi.org/10.1016/0021-9290(90)90054-7

Bergmann, G., Deuretzbacher, G., Heller, M., Graichen, F., & Rohlmann, A. (2001). Hip contact and gait patterns from routine activities, *34*, 859–871. https://doi.org/10.1016/S0021-9290(01)00040-9

Bergmann, G., Graichen, F., & Rohlmann, A. (2004). Hip joint contact forces during stumbling. *Langenbeck's Archives of Surgery*, *389*(1), 53–59. https://doi.org/10.1007/s00423-003-0434-y

Cappozzo, A., Catani, F., Della Croce, U., & Leardini, A. (1995). Position and orientation in space of bones during movement. *Clin. Biomech.*, *10*(4), 171–178. https://doi.org/10.1016/0268-0033(95)91394-T

Chen, S., Andersen, M. S., Rasmussen, J., Tang, W., & County, T. (2013). The effect of muscle setting on kinetics of upper extremity in a baseball pitching modeling: A case study. *ISBS-Conference Proceedings Archive*, *1*(1).

Delp, S. L., Anderson, F. C., Arnold, A. S., Loan, P., Habib, A., John, C. T., … Thelen, D. G. (2007). OpenSim: Open-source software to create and analyze dynamic simulations of movement. *IEEE Transactions on Biomedical Engineering*, *54*(11), 1940–1950. https://doi.org/10.1109/TBME.2007.901024

Delp, S. L. L., Loan, J. P. P., Hoy, M. G. G., Zajac, F. E., Topp, E. L., & Rosen, J. M. (1990). *An interactive graphics-based model of the lower extremity to study orthopedic surgical procedures*. *IEEE transactions on Biomedical Engineering*. Stanford University. https://doi.org/10.1109/10.102791

Dempster, W. T. (1955). *Space requirements of the seated operator : geometrical, kinematic, and mechanical aspects of the body, with special reference to the limbs*. University of Michigan, East Lansing.

Giarmatzis, G., Jonkers, I., Wesseling, M., Van Rossom, S., & Verschueren, S. (2015). Loading of Hip Measured by Hip Contact Forces at Different Speeds of Walking and Running. *Journal of Bone and Mineral Research*, *30*(8), 1431–1440. https://doi.org/10.1002/jbmr.2483

Hamner, S. R., & Delp, S. L. (2013). Muscle contributions to fore-aft and vertical body mass center accelerations over a range of running speeds. *Journal of Biomechanics*, *46*(4), 780–787. https://doi.org/10.1016/j.jbiomech.2012.11.024

Hanavan, E. P. (1964). A Mathematical Model of the human body. *Aerospace Medical Rsearch Laboratories*, 1–149. Retrieved from http://oai.dtic.mil/oai/oai?verb=getRecord&metadataPrefix=html&identifier=AD0608463

Heller, M. O., Bergmann, G., Deuretzbacher, G., Dürselen, L., Pohl, M., Claes, L., … Duda, G. N. (2001). Musculo-skeletal loading conditions at the hip during walking and stair climbing. *Journal of Biomechanics*, *34*(7), 883–893. https://doi.org/10.1016/S0021-9290(01)00039-2

João, F., Ferrer, V., & Veloso, A. (2018). Why abrupt horizontal decelerations can be related to ACL injury? A biomechanical modelling approach based on induced acceleration analysis. *XXVII Isokinetic Medical Group Conference Football*, (June), 3–5.

Lin, Y.-C., Dorn, T. W., Schache, A. G., & Pandy, M. G. (2012). Comparison of different methods for estimating muscle forces in human movement. *Proceedings of the Institution of Mechanical Engineers, Part H: Journal of Engineering in Medicine*, *226*(2), 103–112. https://doi.org/10.1177/0954411911429401

Lu, T. W., & O'Connor, J. J. (1999). Bone position estimation from skin marker co-ordinates using global optimisation with joint constraints. *Journal of Biomechanics*, *32*(2), 129–134. https://doi.org/10.1016/S0021-9290(98)00158-4

Mokhtarzadeh, H., Perraton, L., Fok, L., Muñoz, M. A., Clark, R., Pivonka, P., & Bryant, A. L. (2014). A comparison of optimisation methods and knee joint degrees of freedom on muscle force predictions during single-leg hop landings. *Journal of Biomechanics*, *47*(12), 2863–2868. https://doi.org/10.1016/j.jbiomech.2014.07.027

Pandy, M. G., & Zajac, F. E. (1991). Optimal muscular coordination strategies for jumping. *Journal of Biomechanics*, *24*(1), 1–10. https://doi.org/10.1016/0021-9290(91)90321-D

Pandy, M. G., Zajac, F. E., Sim, E., & Levine, W. S. (1990). An optimal control model for maximum-height human jumping. *Journal of Biomechanics*, *23*(12), 1185–1198. https://doi.org/10.1016/0021-9290(90)90376-E

Renström, P., Arms, S. W., Stanwyck, T. S., Johnson, R. J., & Pope, M. H. (1986). Strain within the anterior cruciate ligament during hamstring and quadriceps activity. *The American Journal of Sports Medicine*, *14*(1), 83–87. https://doi.org/10.1177/036354658601400114

Robertson, D. G. E., Caldwell, G., Hamill, J., Kamen, G., & Whittlesey, S. (2014). *Research Methods in Biomechanics* (2nd ed.). Human Kinetics.

Schache, A. G., Kim, H. J., Morgan, D. L., & Pandy, M. G. (2010). Hamstring muscle forces prior to and immediately following an acute sprinting-related muscle strain injury. *Gait and Posture*, *32*(1), 136–140. https://doi.org/10.1016/j.gaitpost.2010.03.006

Simonsen, E., Dyhre-Poulsen, P., Aagaard, P., Sjøgaard, G., & Bojsen-Møller, F. (1995). Bone-on-bone forces during loaded and unloaded walking. *Cells Tissues Organs*, *152*(2), 133–142.

Thelen, D. G., & Anderson, F. C. (2006). Using computed muscle control to generate forward dynamic simulations of human walking from experimental data. *J Biomech*, *39*(6), 1107–1115. https://doi.org/S0021-9290(05)00099-0 [pii] 10.1016/j.jbiomech.2005.02.010

Thelen, D. G., Anderson, F. C., & Delp, S. L. (2003). Generating dynamic simulations of movement using computed muscle control. *Journal of Biomechanics*, *36*(3), 321–328. https://doi.org/10.1016/S0021-9290(02)00432-3

Veloso, A., João, F., Valamatos, M. J., Cabral, S., & Moniz-Pereira, V. (2015). Subject-specific musculoskeletal model to identify muscle contribution to the acceleration phase in elite sprinting. *33rd Conference of the International Society of Biomechanics in Sports,Pitiers, France*, *33*(1).

Wilk, K. E., Escamilla, R. F., Fleisig, G. S., Barrentine, S. W., Andrews, J. R., & Boyd, M. L. (1996). A comparison of tibiofemoral joint forces and electromyographic activity during open and closed kinetic chain exercises. *American Journal of Sports Medicine*, *24*(4), 518–527. https://doi.org/10.1177/036354659602400418